*Electrochemical and Solid-State Letters*, **14** (10) J69-J72 (2011)
1099-0062/2011/14(10)/J69/4/$28.00 © The Electrochemical Society


# Intense Cyan-Emitting of $Li_2CaSiO_4:Eu^{2+}$ Under Low-Voltage Cathode Ray Excitation

**Mubiao Xie,[a] Hongbin Liang,[a,z] Qiang Su,[a] Yan Huang,[b] Zhenhua Gao,[b] and Ye Tao[b]**

[a]*MOE Laboratory of Bioinorganic and Synthetic Chemistry, State Key Laboratory of Optoelectronic Materials and Technologies, School of Chemistry and Chemical Engineering, Sun Yat-Sen University, Guangzhou 510275, China*
[b]*Beijing Synchrotron Radiation Facilities, Institute of High Energy Physics, Chinese Academy of Sciences, Beijing 100039, China*

$Li_2CaSiO_4$: $Eu^{2+}$ phosphors were prepared using a high temperature solid-state reaction technique. The VUV-vis photoluminescence and low-voltage cathodoluminescence were investigated. The optimal phosphor $Li_2Ca_{0.991}Eu_{0.009}SiO_4$ (LCS-Eu) shows intensive cyan-emitting with color coordinates around (0.119, 0.203) under low voltage cathode ray excitation. Therefore, the color gamut of FEDs is expected to be enlarged by combining this phosphor with RGB tricolor phosphors.
 [DOI: 10.1149/1.3615829] 

Manuscript submitted June 6, 2011; revised manuscript received July 6, 2011. Published July 28, 2011.

As one of promising flat panel displays (FPDs), field emission display (FED) has drawn much attention due to its high brightness, high contrast, light weight, and low power consumption.[1,2] Because FED is an emissive display technology, phosphor plays an important role in the realization of high quality display. Traditionally, sulfide-based phosphors such as $Y_2O_2S$:Eu, Zn(Cd)S:Cu,Au,Al, and ZnS:Ag,Cl often show intensive emission under cathode-ray excitation. These materials have been commercially available red (R), green (G) and blue (B) tricolor phosphors for cathode-ray tubes (CRTs). However, these phosphors are unsuitable for FEDs. CRTs fulfill display through the emission of phosphors under high-voltage and low-current density cathode-ray excitation, but the phosphors produce emitting under low-voltage and high-current density cathode-ray excitation in FEDs. Sulfide-based phosphors are easy to degrade under high energy electron bombardment, and emit sulfide gases leading to cathode poisoning.[3] Tough the main problem of oxide-based phosphors is their relative low light output because their high phonon frequency usually causes high nonradiative relaxation energy loss,[3,4] they are more stable and environmentally friendly in comparison with sulfides. So much attention has been paid to oxide-based phosphors to develop phosphors with high efficiency and good stability under low-voltage electron beam excitation.[1,2,5] In addition, the color gamut of traditional CRT tricolor phosphors is narrow, which is believed to be the disadvantage of full color FEDs.[6] Hence, it is necessary to broaden the color gamut of FEDs by searching appropriate phosphors with proper chromaticity coordinates.

$Eu^{2+}$ ions shows f-d transition in most oxide hosts.[7,8] Luminescence and potential LEDs application of $Li_2CaSiO_4:Eu^{2+}$ have been reported.[9] In addition, the photoluminescence (PL) and decay properties of $Li_2(Sr,Ba,Ca)SiO_4:Eu^{2+}$ phosphors were discussed.[10,11] In this paper, the photoluminescence (PL) and cathodoluminescence (CL) properties of $Li_2CaSiO_4:Eu^{2+}$ under VUV (vacuum ultraviolet) - UV light and low-voltage cathode ray excitations were investigated. The results demonstrated that phosphor $Li_2Ca_{0.991}Eu_{0.009}SiO_4$ (LCS-Eu) shows very intense cyan-emitting with color coordinates around (0.119, 0.203) under low-voltage cathode ray excitation. The color gamut of FEDs is expected to be enlarged by combining this phosphor with RGB tricolor phosphors.

## Experimental

The samples were synthesized using a solid-state reaction technique at high temperature. The starting materials $Li_2CO_3$ (analysis reagent, A.R.), $CaCO_3$ (A.R.), $SiO_2$ (A.R.), $Eu_2O_3$ (99.99%) were weighed stoichiometrically and ground thoroughly in an agate mortar. Then the mixtures were heated at 1073 K for 6 h under a reductive atmosphere ($N_2/H_2 = 3:1$). The final products were cooled down to room temperature (RT) and ground again.

To check the phase purity, powder X-ray diffraction (PXRD) was performed on a Bruker D8 advance X-ray diffractometer with Cu $K_\alpha$ ($\lambda = 1.5405$ Å) radiation at 40 kV and 40 mA. The CL measurements were carried out in an vacuum chamber ($\sim 2 \times 10^{-3}$ Pa), where the phosphors were excited by an electron beam in the voltage range of 0.5–10 kV and different filament currents ($< 2$ mA), and the emission spectra were recorded by a fiber spectrometer (Ocean Optics QEB0388) with a charge-coupled device camera through an optical fiber. The photoluminescence (PL) and photoluminescence excitation (PLE) spectra were recorded on an Edinburgh FLS 920 spectrophotometer, and a 450 W xenon lamp was used as the excitation source. Decay curves were acquired using a time-correlated single photon counting spectrometer with a 450 W nanosecond flash lamp (nF900; channels: 1000; delay time interval: 1.5 ns; pulse frequency: 40 kHz; data acquisition: 3000 counts). The VUV excitation spectra and corresponding emission spectra were measured at the VUV spectroscopy experimental station on beam line 4B8 of Beijing Synchrotron Radiation Facility (BSRF). The measurement details have been described elsewhere.[12]

## Results and Discussion

$Li_2CaSiO_4$ has a body-centered tetragonal unit cell with lattice dimensions $a = 5.047 \pm 0.005$ Å, $c = 6.486 \pm 0.006$ Å and space group $I\bar{4}2m$. In this structure, Ca atoms occupy 8-fold coordination distorted dodecahedral sites.[13,14] The phase purity of all samples was analyzed by XRD measurements. The diffraction of typical sample $Li_2Ca_{0.991}Eu_{0.009}SiO_4$ (b) is plotted in Fig. 1. The XRD patterns of all samples match well with pure $Li_2CaSiO_4$ (a) and JCPDS card 27-0290 ($Li_2CaSiO_4$), indicating that doping of $Eu^{2+}$ ions do not cause significant change in the host structure.

The UV excitation spectrum of LCS-Eu under 520 nm emission at RT is shown in curve b of Fig. 2. To obtain the excitation spectrum in long-wavelength range, here we chose 520 nm as a monitoring emission wavelength, though it deviates from the emission peak (477 nm). Two evident broad bands A and B with maxima at about 303 and 377 nm and a step-like excitation around 450 nm can be seen, respectively, which are assigned to the parity allowed $4f^7(^8S_{7/2}) \rightarrow 4f^6 5d$ transitions of $Eu^{2+}$ ions. The small peaks at about 396, 420 and 460 nm indicate the occurrence of $Eu^{3+}$ ions in the sample.

In order to investigate the absorption behaviors in higher energy range, we also measured the excitation spectrum in VUV range, as shown in curve a of Fig. 2. The peak of band B in curve a shows slight difference with that in curve b due to the different instrumental response of VUV measurements in BSRF and the UV measurements in our laboratory. The weak band C at about 235 nm may also be f-d transition absorption of $Eu^{2+}$. At the same time, we can not exclude the occurrence of $Eu^{3+}$-$O^{2-}$ charge transfer (CT) in this range, because we indeed detected the f-f excitation lines of $Eu^{3+}$ in the sample as mentioned before. The much weak excitation bands

[z] E-mail: cesbin@mail.sysu.edu.cn

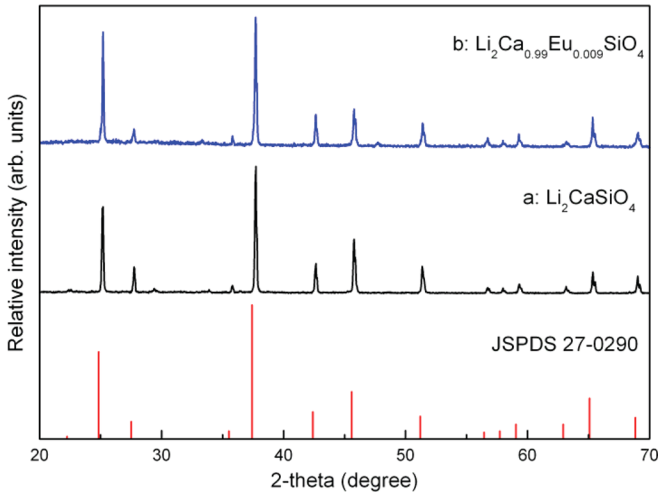


**Figure 1.** (Color online) XRD patterns of samples $Li_2CaSiO_4$ (a) and $Li_2Ca_{0.991}Eu_{0.009}SiO_4$ (b).

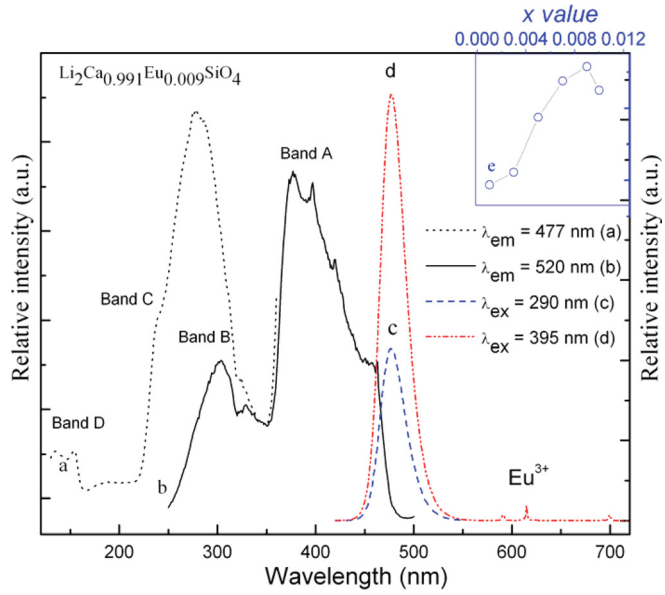


**Figure 2.** (Color online) PLE (a: $\lambda_{em} = 477$ nm, b: $\lambda_{em} = 520$ nm) and PL (c: $\lambda_{ex} = 290$ nm, d: $\lambda_{ex} = 395$ nm) spectra of LCS-Eu phosphor. The inset curve e shows the dependence of PL intensity on $Eu^{2+}$ concentration ($\lambda_{ex} = 290$ nm, the integrated wavelength 430–550 nm).

below 200 nm are due to host-related absorptions, showing that the energy transfer (ET) efficiency between host and $Eu^{2+}$ is inefficient.

Upon 290 nm excitation, as shown in Fig. 2c, the phosphor LCS-Eu shows a broad band emission with a maximum at about 477 nm which can be unambiguously assigned to $4f^65d^1 \rightarrow 4f^7$ transition of $Eu^{2+}$. The emission intensity of $Eu^{2+}$ as function of $Eu^{2+}$ concentration ($x$) is shown in inset curve e of Fig. 2. It is found that the concentration quenching occurs when $Eu^{2+}$ concentration at $x = 0.009$, that is to say, the optimum phosphor is $Li_2Ca_{0.991}Eu_{0.009}SiO_4$, we shorten it as LCS-Eu in this paper.

The occurrence of $Eu^{3+}$ in the sample LCS-Eu can be further confirmed by emission spectrum (curve d). At the moment, we chose 395 nm as excitation wavelength, because $Eu^{3+}$ often shows intense $^7F_0$-$^5L_6$ absorption around this wavelength.[15] Upon 395 nm excitation, weak peaks at 591, 613 and 700 nm due to the $^5D_0$-$^7F_j$ transitions of $Eu^{3+}$ ions can be clearly seen. In fact, $Eu^{3+}$ ions are difficult to be totally reduced to $Eu^{2+}$ ions under a reductive atmosphere ($N_2$-$H_2$ mixture) during our experiment. Here, an approach is adopted to predict the stability of $Eu^{2+}$ in the crystal. As shown in the Eq. 1, the valence $V_i$ (the oxidation number) of an atom is equal to the sum of the individual bond valences (BVS) coordinating the atom[16]

$$V_i = \sum_j \exp[(R_o - R_{ij})/b] \qquad [1]$$

where $R_{ij}$ is the observed bond length in the crystal structure,[17] $R_0$ is a tabulated parameter and equals to 2.147 Å for Eu(II)-O bond, and b is an empirical constant 0.37 Å. Considering the $R_{ij}$ values as 2.40 and 2.69 Å according to the $Li_2CaSiO_4$ crystal structure,[12] we can obtain a $V_i$ value of 2.15. This value is larger than its formal charge (+2), indicating that the stability of $Eu^{2+}$ ions in this compound may be low during the synthesis process.

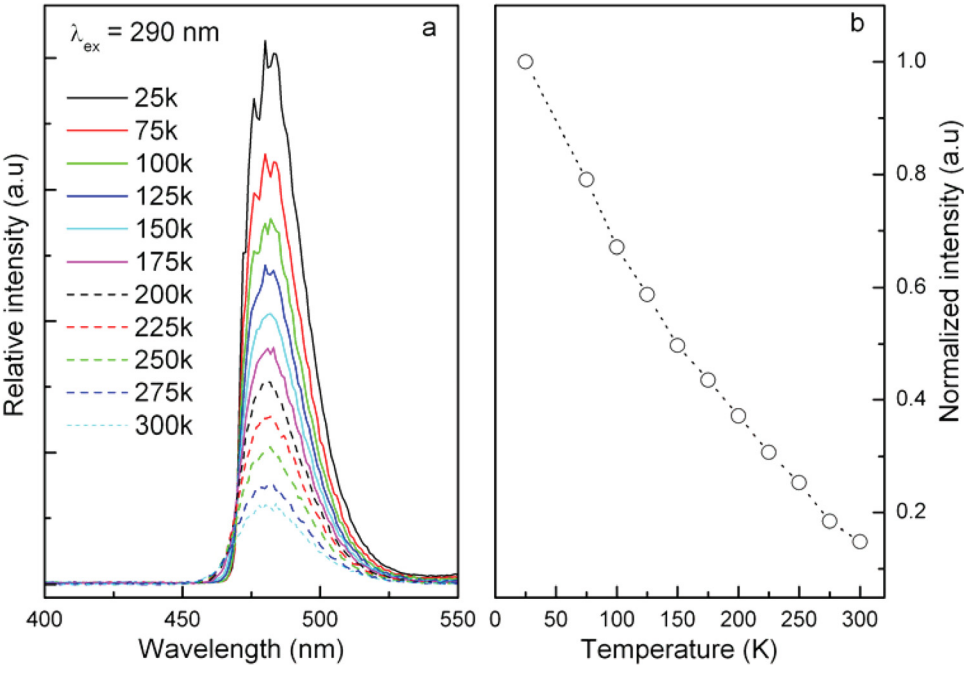


**Figure 3.** (Color online) (a) The emission spectra of LCS-Eu under 290 nm excitation at different temperatures. (b) The dependence of the integral emission intensity of the sample LCS-Eu on temperature.

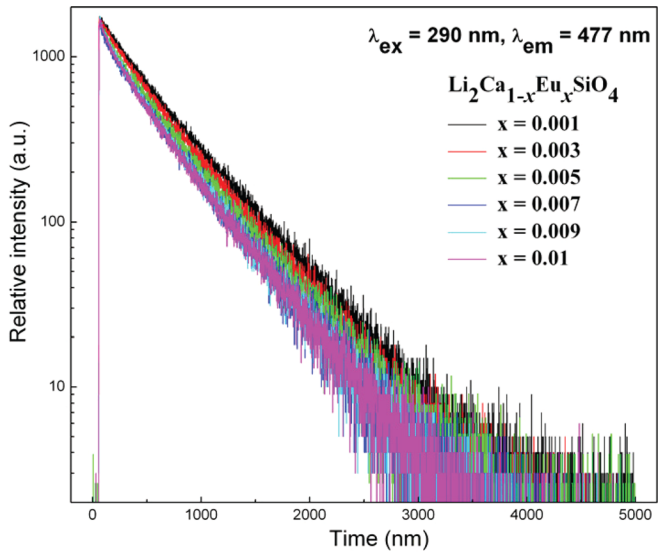


**Figure 4.** (Color online) Decay curves of the emission at 477 nm of $Li_2Ca_{1-x}Eu_xSiO_4$ upon excitation at 290 nm.

Figure 3a shows the emission spectra of the sample LCS-Eu under 290 nm excitation in the temperature range from 25 to 400 K. Figure 3b represents the dependence of the integral emission intensity on temperature. The position of the emission maximum nearly keeps invariable with increasing of temperature. The emission intensity of $Eu^{2+}$ gradually decreases with the increase of temperature due to thermal quenching.

The decay curves of the $Eu^{2+}$ emission at 477 nm under 290 nm excitation at RT are presented in Fig. 4. The decays are nearly single exponential but with different lifetime values. The lifetime values decrease gradually from 495 to 378 ns with increasing of $Eu^{2+}$ doping concentration. This is due to increasing of the migration of energy nonradiatively between the $Eu^{2+}$ ions.

The cathodoluminescence (CL) spectrum of optimum phosphor LCS-Eu under a low voltage electron beam (100 μA, 4 kV) excitation was measured at RT, as shown in curve a of Fig. 5. A broad band with maximum peak at about 480 nm can be observed, which

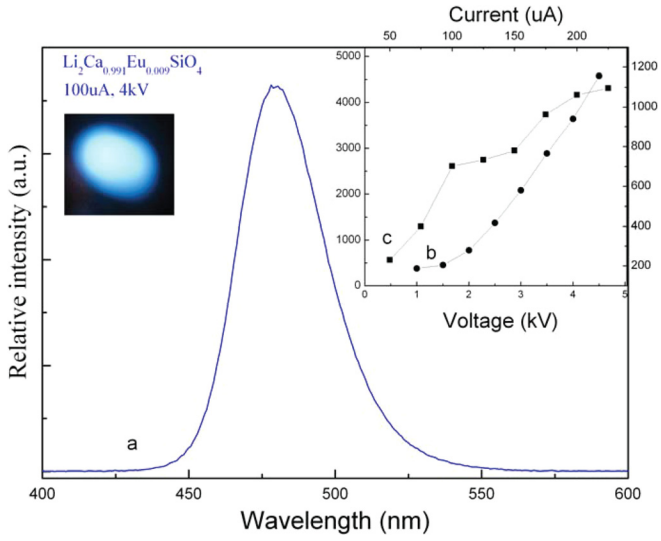


**Figure 5.** (Color online) Cathodoluminescence emission spectrum (Current = 100 μA, Voltage = 4 kV) of sample LCS-Eu. Left inset is the relevant luminescent photograph. Right inset is CL intensity as a function of accelerating voltages and filament currents.

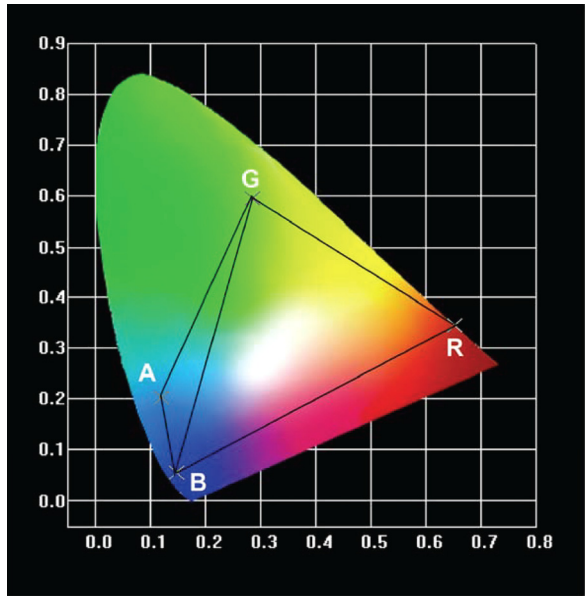


**Figure 6.** (Color online) CIE chromaticity diagram for phosphor LCS-Eu (A) under 100 μA, 4 kV excitation together with the commercial tricolor phosphors $Y_2O_2S$: Eu (R), ZnS: Cu,Au,Al (G) and ZnS: Ag,Cl (B).

is similar with that in Fig. 2. The relevant luminescence photograph is displayed in the left inset of Fig. 5, which shows very intense cyan-emitting.

The right inset of Fig. 5 displays the typical cathodoluminescence emission intensity of LCS-Eu phosphor as a function of accelerating voltages and filament currents. When the filament current is fixed at 100 μA, with the increase of accelerating voltage from 1 to 4.5 kV, the cathodoluminescence intensity almost linearly increases (curve b). The same phenomenon occurs for the dependence of filament current when the voltage is fixed at 2 kV. Under 2 kV voltage excitation, the cathodoluminescence intensity gradually increases with increasing of filament current from 25 to 225 μA (curve c). These properties indicate that the phosphor LCS-Eu is resistant to the current saturation, which is in favor of FEDs application.

To our knowledge, the most commonly used cathode-ray phosphors are $Y_2O_2S$: Eu (red), ZnS: Cu,Au,Al (green) and ZnS: Ag,Cl (blue). However, the color gamut of these tricolor phosphors is narrow. The color coordinates of above commercial red (R), green (G), blue (B) phosphors and LCS-Eu (A) are shown in Fig. 6. We can see that LCS-Eu phosphor exhibits cyan-emitting color with color coordinates (0.119, 0.203), which is on the outside of the traditional color gamut. Hence, the color gamut of FEDs is expected to be enlarged by combining this phosphor with RGB tricolor phosphors. In consideration of the excellent luminescence properties, i.e. very intense cyan-emitting under low-voltage cathode ray excitation, the fabrication of FEDs with broadened color gamut using this phosphor is underway.

In summary, the VUV-vis photoluminescence and low-voltage cathodoluminescence of $Eu^{2+}$ doped $Li_2CaSiO_4$ phosphors were investigated, revealing that $Eu^{2+}$ ions show emission at 477 nm. The optimal phosphor LCS-Eu has a very intense cyan-emission and with color coordinates (0.119, 0.203) under low voltage cathode ray excitation, which can enlarge the color gamut of FEDs, demonstrating the potential application in FEDs.

## Acknowledgments

The work is financially supported by National Basic Research Program of China (973 Program, Grant No. 2007CB935502), National Natural Science Foundation of China (Grant Nos. 20871121 and 10979027), Natural Science Foundation of Guangdong Province (Grant No. 9151027501000003), and the Yat-sen Innovative Talents Cultivation Program for Excellent Tutors.

## References


1. X. M. Liu and J. Lin, *J. Mater. Chem.*, **18**, 221 (2008).
2. W. P. Chen, H. B. Liang, B. Han, J. P. Zhong, and Q. Su, *J. Phys. Chem. C*, **113**, 17194 (2009).
3. V. A. Bolchouchine, E. T. Goldburt, B. N. Levonovitch, V. N. Litchmanova, and N. P. Sochtine, *J. Lumin.*, **87–89**, 1277 (2000).
4. R. X. Yan and Y. D. Li, *Adv. Funct. Mater.*, **15**, 763 (2005).
5. G. Jia, Y. H. Song, M. Yang, Y. J. Huang, L. H. Zhang, and H. P. You, *Opt. Mater.*, **31**, 1032 (2009).
6. P. H. Holloway, T. A. Trottier, B. Abrams, C. Kondoleon, S. L. Jones, J. S. Sebastian, and W. J. Thomes, *J. Vac. Sci. Technol. B*, **17**, 758 (1999).
7. Y. C. Chiu, W. R. Liu, C. K. Chang, C. C. Liao, Y. T. Yeh, S. M. Jang, and T. M. Chen, *J. Mater. Chem.*, **20**, 1755 (2010).
8. W. Lu, Z. D. Hao, X. Zhang, Y. F. Liu, Y. S. Luo, X. Y. Liu, X. J. Wang, and J. H. Zhang, *J. Electrochem. Soc.*, **158**, H124 (2011).
9. J. Liu, J. Y. Sun, and C. S. Shi, *Mater. Lett.*, **60**, 2830 (2006).
10. C. Kulshreshtha, N. Shin, and K. S. Sohn, *Electrochem. Solid-State Lett.*, **12**, J55 (2009).
11. C. Kulshreshtha, A. K. Sharma, and K. S. Sohn, *J. Electrochem. Soc.*, **156**, J52 (2009).
12. Y. Tao, Y. Huang, Z. H. Gao, H. Zhuang, A. Y. Zhou, Y. L. Tan, D. W. Li, and S. S. Sun, *J. Synchrotron Radiat.*, **16**, 857 (2009).
13. P. Dorenbos, L. Pierron, L. Dinca, C. W. E. van Eijk, A. Kahn-Harari, and B. Viana, *J. Phys.: Condens. Matter*, **15**, 511 (2003).
14. J. A. Gard and A. R. West, *J. Solid State Chem.*, **7**, 422 (1973).
15. W. P. Chen, H. B. Liang, M. B. Xie, and Q. Su, *J. Electrochem. Soc.*, **157**, J21 (2010).
16. V. P. Dotsenko, S. M. Levshov, I. V. Berezovskaya, G. B. Stryganyuk, A. S. Voloshinovskii, and N. P. Efryushina, *J. Lumin.*, **31**, 311 (2011).
17. N. E. Brese and M. O'Keeffe, *Acta Crystallogr.*, **B47**, 192 (1991).